JOURNAL OF AIRCRAFT
Vol. 31, No. 1, Jan.–Feb. 1994

Static and Dynamic Coefficients of a Cross-Type Parachute

Zalman Shpund* and Daniel Levin†
Technion—Israel Institute of Technology, Haifa 32000, Israel

A parametric investigation of the aerodynamic characteristics of a group of cross-type parachutes is described. The investigation includes the measurements of the static and dynamic aerodynamic coefficients, utilizing a measuring system designed especially for this task. The validity of the measuring technique was established by comparing the results to previous data. The static aerodynamic coefficients are presented as a function of the angle of attack and the parachute geometric parameters. Spin is introduced by staggering the length of the cords. The effects of the spin on the axial force, as well as on the stability parameters, are investigated with different parachute geometries. The measurements show an increase of up to 50% in the axial force due to the spin, followed by a decrease in the longitudinal stability, which explains the tendency for this type of parachute to undergo a conning motion during descent flight. The apparatus supplies a unique means to measure the maximum obtainable roll rate and the maximum torque the cords can transfer before collapsing.

Nomenclature

Cl_p = roll damping coefficient, $\partial Cl/\partial[p(d/2V)]$
Cl_s = induced roll coefficient
Cmref = restoring moment coefficient
Cnor = normal force coefficient
Cr = measured roll moment coefficient
Cxtot = axial force coefficient
D_{ref} = reference length, d
d = parachute's spread diameter, m
L = parachute's lobe length, m, Fig. 1
l = cord length, m
p = roll rate, rpm
R = deployed canopy radius, m, Fig. 4
V = air velocity, m/s
W = parachute's lobe width, m, Fig. 1
X = length, m, Fig. 4
α = angle of attack, deg

Introduction

SOME modern decelerating devices are designed to perform tasks that are beyond the traditional function of decreasing the flight velocity of a payload (e.g., an airplane, a projectile, a smart submunition). These devices, including various types of parachutes, have become aerodynamic means for controlling the trajectories of the payloads; they introduce maneuvers such as gliding, rotating, or a combined motion pattern (e.g., conical spin). These decelerators can be remotely controlled in real time, as well as predesigned to carry out a specific mission. Prediction of the trajectory, as well as the dynamic behavior during flight, of the aerodynamic decelerated system (i.e., parachute and payload) can be determined by simulation codes similar to those used for rigid configurations.[1,2] These codes most commonly assume that the aerodynamic system behaves aerodynamically like a rigid body, which could be defined by its aerodynamic coefficients and physical properties. These coefficients include the static and dynamic characteristics of the configurations, and are typically nonlinear with the angle of attack. In the past, one could measure the static coefficient[3–5] in a wind tunnel, and obtain the dynamic ones from drop tests. Drop tests are very expensive, are limited by the difficulty in controlling the test variables, and have low accuracy. An attempt to measure the roll rate of cross-type parachutes in order to explain their tendency to rotate in flight can be seen in the research results presented in Ref. 6. In this work, the spin of the canopy was induced by staggering the cords of the parachute, and the roll rate was measured as a function of the stagger ratio, the number of cords, and the canopy geometry. This method of inducing spin to the canopy was adopted in the present study. Several stagger ratios were used to change the spin rates of the canopy.

The idea of using a multiple support rather than a single one for a parachute model in wind-tunnel tests was first suggested by Doherr and Schmerwitz[4] in their work on measuring the static aerodynamic coefficients. A similar approach could be used for dynamic measurements also. The system used in the current study (a modified version of that used in Ref. 7) introduces a sophisticated spin-measuring device that also includes a pneumatically controlled braking system. With the help of advanced balances (compared to those of Doherr and Schmerwitz[4]), both the static and the dynamic characteristics of the cross-type rotating parachute models could be measured accurately. Comparisons with previous data from wind-tunnel testing was limited to the nonspinning cases only, since no dynamic wind-tunnel data was available.

Experimental Setup

Wind Tunnel

The experiments were conducted in the subsonic wind-tunnel laboratories at the Aeronautical Research Center at the Technion Institute in Haifa. This is a 1- × 1-m² cross section, subsonic wind tunnel. It is an open-return-type tunnel with a contraction ratio of 25:1 and a top speed of 35 m/s. All the tests were conducted at a constant speed of 20 m/s, which is a typical speed for the parachute models.

Measuring Apparatus

The measuring apparatus is based on a double-strut suspension system. The front support contains the forward six-component balance, and is attached to the spin-measuring and control system. The latter is shaped like a typical payload configuration to simulate the aerodynamic payload-parachute interaction. The back strut contains the second balance and the canopy support system. A brief description of the measuring apparatus and the calibration process is given in Ref.

Received Feb. 18, 1992; revision received Oct. 25, 1992; accepted for publication Nov. 19, 1992.

*Research Engineer, Aerodynamic Research Center, Faculty of Aerospace Engineering. Member AIAA.
†Senior Research Fellow, Faculty of Aerospace Engineering. Member AIAA.

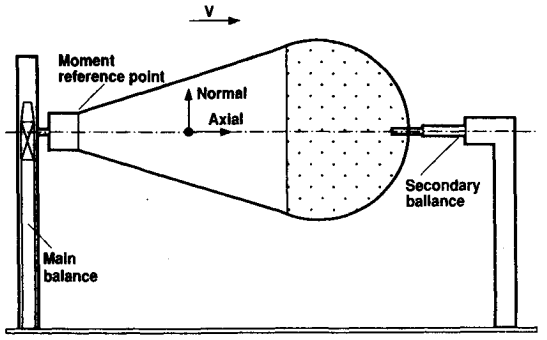

Fig. 1 Schematic of the test setup and axis system.

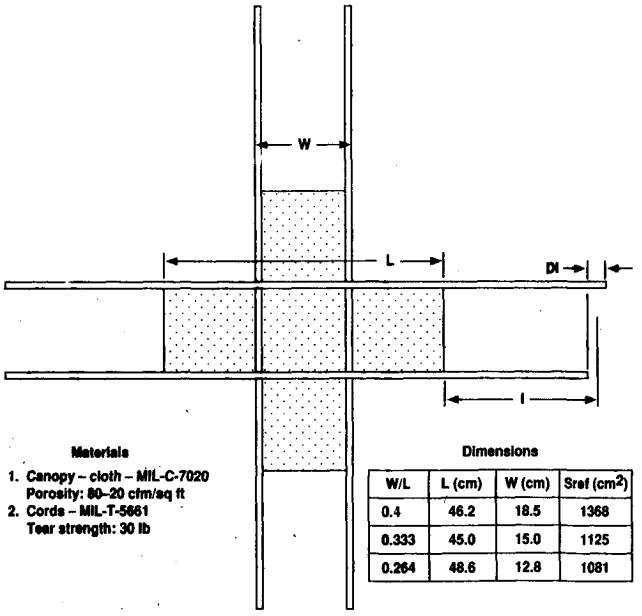

W/L	L (cm)	W (cm)	Sref (cm^2)
0.4	46.2	18.5	1368
0.333	45.0	15.0	1125
0.264	48.6	12.8	1081

Fig. 2 Geometric dimensions of the wind-tunnel models.

7. A schematic description of the test setup, the reference dimensions, and the axis measuring system is shown in Fig. 1.

Parachute Models

All the parachute models tested in this research were cross-type parachutes. They differed in their typical dimensions, W and L. A diagram of the canopy models (geometric dimensions and materials) is provided in Fig. 2. The spin was induced by staggering the length of the cords attached to each lobe of the canopy, as shown in Fig. 2. Three stagger ratios ($\Delta l/L$) were used, 0 for the nonrotating models, and 0.05 and 0.1 for the rotating models.

Test Results

Nonrotating Parachutes

Axial Force

In Fig. 3 the axial force coefficients are presented as a function of angle of attack, with the canopy aspect ratio as a parameter, for the nonrotating models tested. The results are shown in two graphs; the upper one for a cord length $l = L$ (Fig. 2) and the lower one $l = 0.7L$. The latter one was checked to improve the rotating moment transferability. As can be seen, there is an increase in axial force with increase in the canopy aspect ratio and cord length. The increase in axial force as a result of the increase in aspect ratio is to be expected, since an increase in aspect ratio means a decrease in the geometric porosity of the canopy.[4] The decrease in axial force as a result of decrease in cord length is due to changes in the equilibrium state of the forces governing the canopy deployment pattern as shown in Fig. 4.

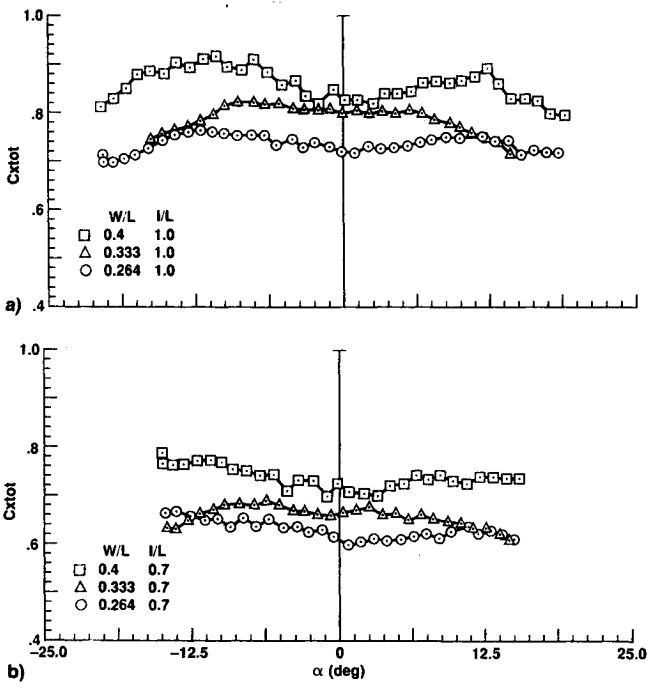

Fig. 3 Axial force coefficients as a function of angle of attack: a) cord length $l = L$ and b) cord length $l = 0.7L$.

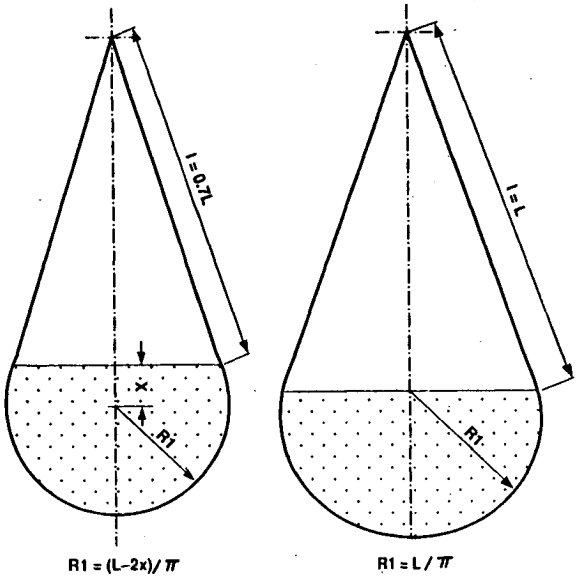

Fig. 4 Schematic description of the deployed canopy shape patterns as the cord length is changed.

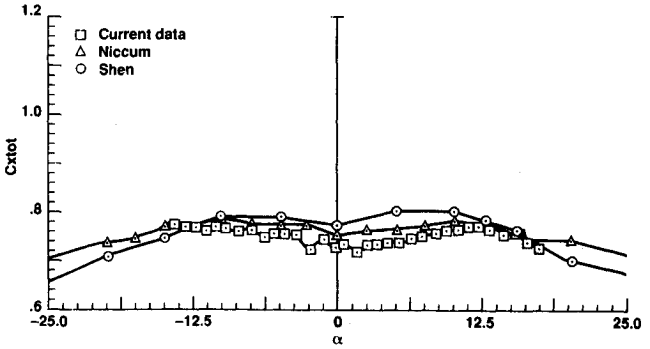

Fig. 5 Comparison of the current results with earlier research for nonrotating canopies.

A comparison of the axial force coefficients in the present study and in previous tests is presented in Fig. 5. Data is shown for a configuration, with $W/L = 0.333$. Although the test setups are considerably different from each other, and there is support interference that varies from one setup to the other, there is good agreement between the two data sets.

Normal Force and Center of Pressure

Typical results for the normal force coefficient as a function of angle of attack (Fig. 6) are compared with previous work in Fig. 7. The repeatability of the force measurement was in the order of 1%, and the accuracy of the measurement was better than 0.5%. One can see from this figure that there is good agreement between the present results and those presented by Shen and Cockrell.[5] The comparison with Niccum et al.[3] data shows similarity in the trends, but poorer agreement. An explanation of this inconsistency is believed to lie in the differences between the different test setups. In Niccum's work, the forces acting on the central rod might have been included in the measurement. The test setup in Shen and Cockrell's work is more like the one in the present work, and so are the results.

Figure 7 presents the center-of-pressure (c.p.) location *Xcp*, a parameter which gives an indication of the longitudinal stability. The accuracy of the calculations of the slope at zero angle of attack was better than 2%. As expected, the low-aspect-ratio models tend to be more stable.[4] The results presented in Fig. 7 indicate that the configurations with the longer cords are significantly more stable than those with shorter cords.

Rotating Parachutes

Steady-State Spin Rate

Typical results for the steady-state spin rate as a function of angle of attack are presented in Fig. 8. As can be seen, there is only a slight dependence of spin rate on angle of attack. In the following discussions, spin rate is regarded as independent of the angle of attack. The measurement of the spin rate had an accuracy of 0.5%.

The results presented in Fig. 9 summarize the dependence of spin rate (nondimensional) at zero angle of attack on canopy aspect ratio, with the cord length and stagger ratio ($\Delta l/L$) as parameters. There is a slight effect of the aspect ratio on the spin rate, and a maximum spin rate at an aspect ratio of 0.33. This is more evident for the case with short cords. As expected, a slightly higher spin rate is obtained when the cords are shortened. This could also be the result of the shorter cords having a larger $\Delta l/L$.

A change of the stagger ratio from $\Delta l/L = 0.05$ to $\Delta l/L = 0.10$, leads generally to an increase in the spin rate. However, this increase is much more pronounced in the case of the short cord configuration, where there is a growing trend of spin rate increase in W/L, the added spin rate varying from 5 to 25%. In the case of the long cords, there was an increase in spin rate for $W/L = 0.33$, and no change, or even a slight decrease, for other aspect ratios. Similar tests were conducted by Doherr and Synofzik,[8] where the rotor quality of several types of parachutes was investigated. One of their models was a cross-type parachute, however, there is not enough data regarding the parachute to enable a direct comparison of the data. The rotor quality of their cross-type model was 0.17, while in the current test the rotor quality range depending on the parachute aspect ratio and cord length varied from 0.156 to 0.26. One can conclude that the spin rate is strongly affected by the stagger ratio, at small $\Delta l/L$ (<5%), whereas at larger stagger ratios there is a dependence on a combination of parameters such as aspect ratio, cord length, and stagger ratio that simultaneously affect the spin rate.

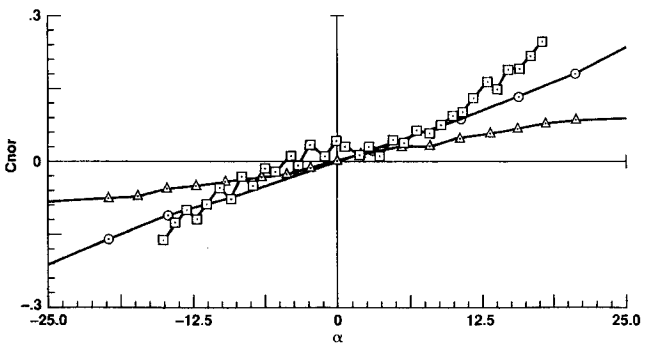

Fig. 6 Normal force coefficients vs angle of attack—a comparison with earlier data.

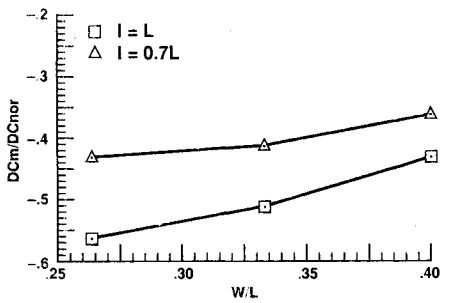

Fig. 7 Center-of-pressure location (*Xcp*). Nonrotating parachute models.

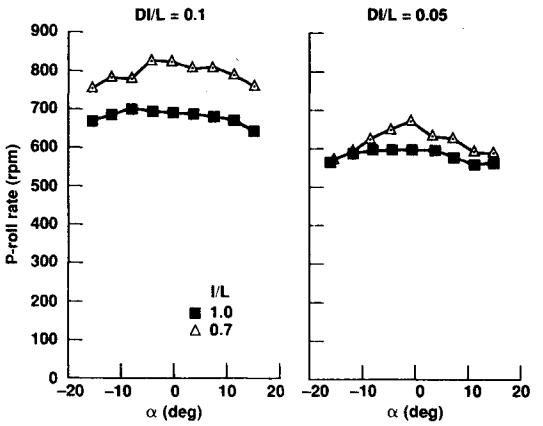

Fig. 8 Steady-state spin rate vs angle of attack.

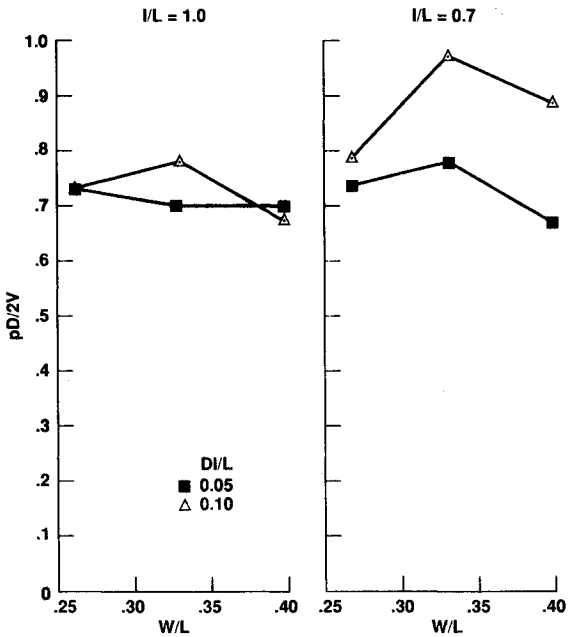

Fig. 9 Nondimensional spin rate at zero angle of attack, as a function of canopy aspect ratio.

Axial Force

Results of *Cxtot* are presented in Fig. 10 as a function of angle of attack and with the stagger ratio as a parameter. The results shown are for the $W/L = 0.4$ configuration; the two graphs represent two different cord lengths. *Cxtot* is almost independent of the angle of attack (in the region tested), except for the nonrotating case, where there is a local minimum at zero angle of attack. In the case of the rotating parachutes, because of the rotational forces, the effect of the angle of attack on the shape of the canopy is much smaller than in the nonrotating case, and the effect of the angle of attack on the axial force becomes negligible. The value of the axial force coefficient at zero angle of attack could be used as representative of the force at all angles. The effect of the stagger ratio on the axial force is obviously big. By inducing spin, and thereby affecting the canopy's shape, the stagger ratio increases the axial force dramatically (additions of up to 50% were recorded). However, it is interesting to note that this addition is not linear, although it is monotonic, and that changing from a stagger ratio of $\Delta l/L = 0.05$ to $\Delta l/L = 0.1$ leads to a smaller change in the case of the long cords, whereas a similar change in the stagger ratio leads to a larger drag increase for a configuration with short cords.

Axial-force-coefficient variation with the canopy aspect ratio is presented in Fig. 11, with the stagger ratio as a parameter. It is evident that within the range tested, an increase in stagger ratio always caused an increase in the axial force. However, the amount of this increase varied for the different aspect ratios and the different cord lengths. In general, the addition to the axial force was larger for the parachutes with the short cords, as in both cases there is a similar maximum force, whereas the axial force for the nonrotating parachutes is larger for the longer cord configuration at zero stagger. As expected, the effect of an increase in the canopy aspect ratio is to decrease the geometric porosity, and therefore, to increase the axial force.

Stability and Slide Forces

The slope of the curve of the restoring moment (*Cmref*) in the pitch plane, as a function of the normal force (*Cnor*) in the same plane, indicates the location of the c.p., *Xcp*. Typical results for the restoring moment coefficient, measured at the center of gravity (c.g.), are presented in Fig. 12. One can see

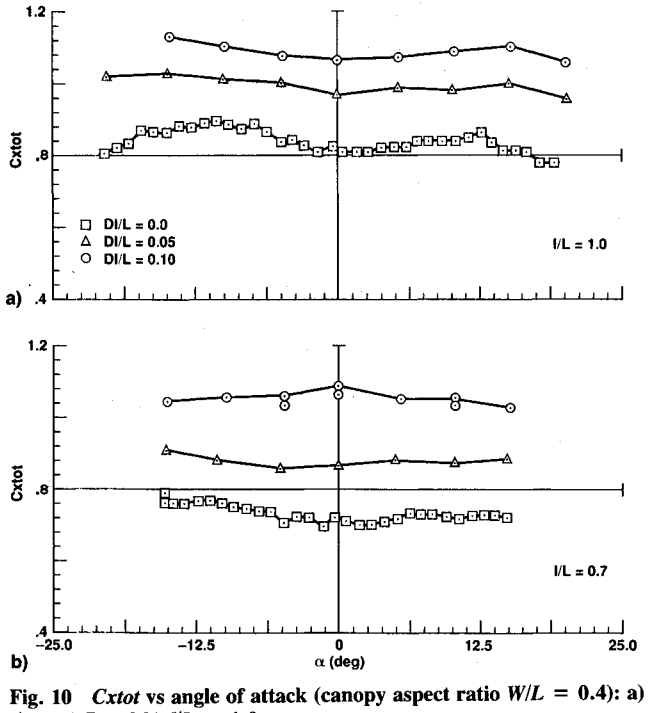

Fig. 10 *Cxtot* **vs angle of attack (canopy aspect ratio $W/L = 0.4$): a) $l/L = 0.7$ and b) $l/L = 1.0$.**

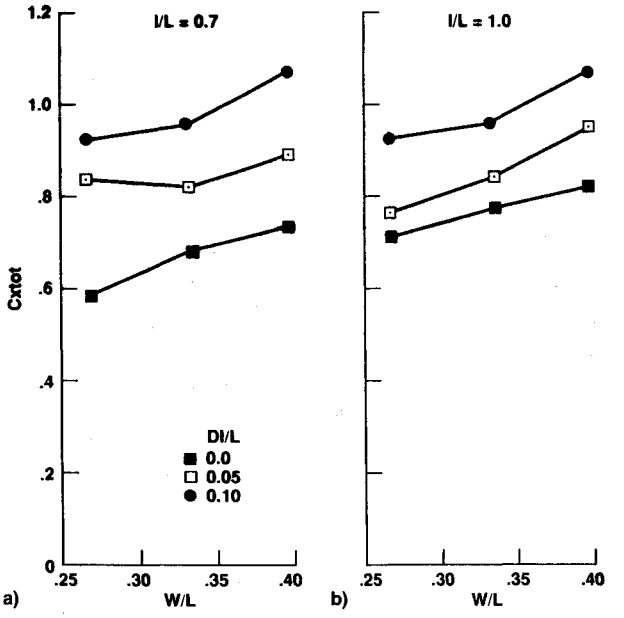

Fig. 11 *Cxtot* **as a function of the canopy aspect ratio, W/L: a) $l/L = 0.7$ and b) $l/L = 1.0$.**

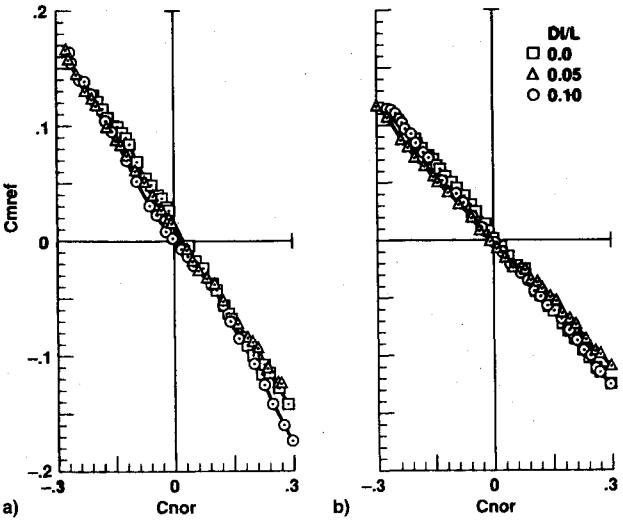

Fig. 12 *Cmref* **vs normal force coefficients, $W/L = 0.264$: a) $l/L = 0.7$ and b) $l/L = 1.0$.**

the almost linear dependency between the coefficients (*Cmref* and *Cnor*), which indicates that, although the behavior of the longitudinal coefficients is not linear with the angle of attack, the c.p. location is independent of the angle of attack.

In Fig. 13, the location of the c.p. as a function of the canopy aspect ratio is presented for all the configurations tested. When calculated relative to the c.g., a negative value for the *Xcp* indicates a stable payload-parachute configuration. Three general trends can be observed:

1) The configurations with the longer cords are more stable, as expected, since the canopy is farther away from the payload; however, the motion in the *Xcp* location is smaller than the addition in the cord length.

2) In the case of rotating parachutes, stability decreases with increasing aspect ratio of the canopy. This is not always the case for the nonrotating parachute. This effect could be related to the changes in the canopy shape as a function of aspect ratio and spin rate. However, this effect is not even a monotonic one, as shown in Fig. 13.

3) Spinning reduces the stability of the parachute in most of the test cases. However, the parachutes with the larger stagger ratio were more stable than those with the smaller one, and in some cases more stable than the nonrotating

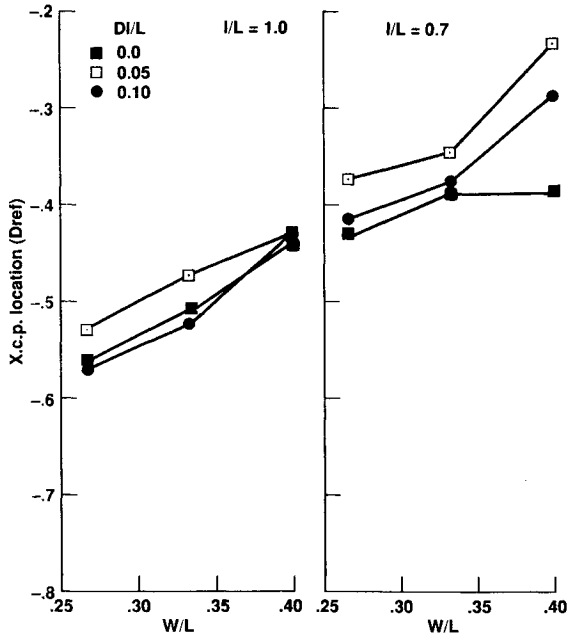

Fig. 13 Location of *Xcp*.

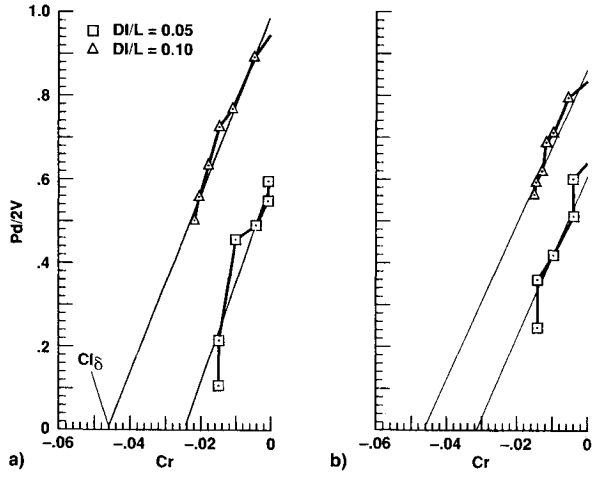

Fig. 14 Typical calculation of the rolling coefficients, $W/L = 0.4$: a) $l/L = 0.7$ and b) $l/L = 1.0$.

parachutes. It is possible that there is an effect caused by Magnus forces on the forward part of the parachute, moving the c.p. forward.

Rolling Coefficients

The technique to obtain the rolling coefficients (i.e., the roll inducing and the roll-damping moment coefficients) is described in Ref. 1. When a partial braking moment is applied to the bearing system in the forebody, the spin rate decays, as a function of the torque, and the balance reads the overall roll moment (friction- and brake-induced moment). When the nondimensional spin rate ($Pd/2V$) is plotted against the measured roll moment (Fig. 14), a linear relation is expected, at least in the range before the collapse of the cords. This straight line can be continued to the "theoretical point," where it intersects the zero-roll-rate axis. This point stands for the rolling moment (Cl_δ) that the parachute would have exerted—were it free to roll—at zero-roll rate. Another important feature is the slope of this line, which is related to Cl_p of the revolving parachute. The calculations of Cl_p and Cl_δ are based on a small number of data points, even though, the accuracy for the dynamic coefficients is acceptable. The standard deviation of Cl_p is 5%, and of Cl_δ is 2.5%. It is evident that, for the results for the parachute with aspect ratio $W/L = 0.4$, there is no effect of stagger ratio or cord length on the damping. The differences between the configurations lie in the maximum roll rate, the maximum transferable moments as indicated by the position where the cords collapse, and in the roll inducing moments.

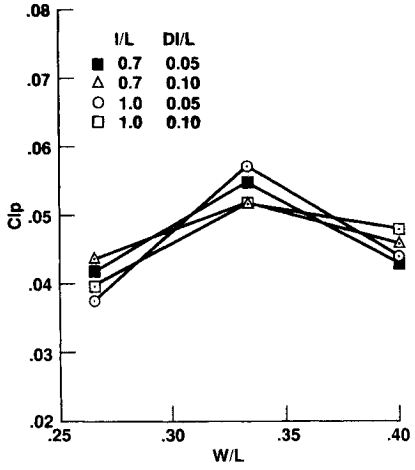

Fig. 15 Roll-damping coefficient as a function of the canopy aspect ratio.

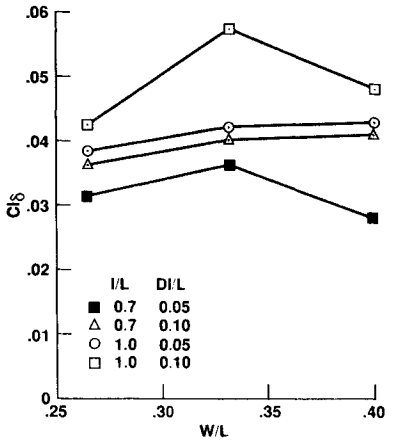

Fig. 16 Roll-inducing moment as a function of the canopy aspect ratio.

The effect of the aspect ratio on roll damping is presented in Fig. 15. It shows that there exists an optimal damping for $W/L = 0.33$. The effects of the cord length, as well as the stagger ratio, are small and inconsistent. This is not the case for the roll-inducing moment (Fig. 16); there is a definite effect of the stagger ratio and the cord length. The higher the length or stagger ratio, the higher the moment. The aspect ratio of $W/l = 0.33$ seems to generate a higher moment than either of the other aspect ratios.

Conclusions

An experimental parametric study of the aerodynamic qualities of cross-type parachutes was conducted in a subsonic wind tunnel, utilizing a new experimental technique. The static aerodynamic coefficients of several configurations were in good agreement with available data, and helped to validate the experimental technique used in this study. Two configuration parameters varied in the static tests: 1) the canopy aspect ratio and 2) the cord length. Both parameters had a similar effect on the drag measurement; any increase in either of them increased the effective blocking area, and hence, the axial force. However, they differed in their effect on the stability of the parachutes. The c.p. moved backward (more stable) with increasing cord length, and forward with increasing aspect ratio. The dynamic tests introduced a third parameter, the stagger ratio of the cords. This parameter signifies the twist that is introduced to the tip of the parachute lobes,

which causes the driving roll moment. The stagger ratio has a strong effect on the spin rate obtained by the parachute, and on the addition to the axial force due to spin. This addition to the axial force is higher in the case of the short cords, and can be as much as a 50% increase. The effect of the stagger ratio on the roll-damping qualities of the parachute is negligible, whereas the effect on the longitudinal stability depends on the parachute's aspect ratio and cord length.

The results of these tests are in agreement with drop test data. However, there is a need for more tests to fully understand the aerodynamics of a parachute-payload configuration. The effect of the payload size and the interaction between the payload wake and the flow around the parachute should be investigated, as well as different canopy configurations and materials.

References

[1]Ewing, E. G., "Deployable Aerodynamic Deceleration Systems," NASA SP-8066, Washington, DC, April 1971.

[2]Doherr, K. F., and Schilling, H., "9DOF-Simulation of Rotating Parachute Systems," *Proceedings of the 11th AIAA Aerodynamic Decelerator Systems Technology Conference* (San Diego, CA), April 9–11, 1991, pp. 333–343 (AIAA Paper 91-0877).

[3]Niccum, R. J., Haak, E. L., and Gutencauf, R., "Drag and Stability of Cross Type Parachutes," FDL-TDR-64-155, Univ. of Minnesota, Minneapolis, MN, Feb. 1965.

[4]Doherr, K. F., and Schmerwitz, D., "Measurements for Rigid Parachute Models," Royal Aeronautical Society Symposium on Parachutes and Related Technologies, London, Sept. 1971.

[5]Shen, C. Q., and Cockrell, D. J., "Aerodynamic Characteristics and Flow Round Cross Parachutes in Steady Motion," AIAA Paper 86-2473, Oct. 1986.

[6]Frucht, Y. I., "Models of Three Dimensional Motion of a Pin Jointed Parachute-Payload System," Dept. of Engineering, Leicester Univ., Leicester, England, UK, 1987.

[7]Shpund, Z., and Levin, D., "Improved Measurements of the Dynamic Loads Acting on Rotating Parachutes," AIAA Paper 86-2473, Oct. 1986.

[8]Doherr, K. F., and Synofzik, R., "Investigation of Rotating Parachutes for Submunition," AIAA Paper 86-2438, Oct. 1986.